Environ. Sci. Technol. **2002**, *36,* 4302−4311

Reactions of Hydroxyl Radicals and Ozone with Acenaphthene and Acenaphthylene

FABIENNE REISEN†,§ AND
JANET AREY*,†,‡,§

Air Pollution Research Center, Interdepartmental Program in Environmental Toxicology, and Department of Environmental Sciences, University of California, Riverside, California 92521

Acenaphthene and acenaphthylene are polycyclic aromatic hydrocarbons (PAHs) emitted into the atmosphere from a variety of incomplete combustion sources such as diesel exhaust. Both PAHs are present in the gas phase under typical atmospheric conditions and therefore can undergo atmospheric gas-phase reactions with the hydroxyl (OH) radical and for acenaphthylene with ozone. Using a relative rate method, rate constants have been measured at 296 ± 2 K for the OH radical reactions with acenaphthene and acenaphthylene of (in units of 10^{-11} cm^3 molecule^{-1} s^{-1}) 8.0 ± 0.4 and 12.4 ± 0.7, respectively, and for the O_3 reaction with acenaphthylene of $(1.6 \pm 0.1) \times 10^{-16}$ cm^3 molecule^{-1} s^{-1}. The products of the gas-phase reactions of acenaphthene and acenaphthylene and their fully deuterated analogues have been investigated using in situ atmospheric pressure ionization tandem mass spectrometry (API-MS) and gas chromatography-mass spectrometry (GC-MS). The major products identified from the OH radical-initiated reaction of acenaphthene and acenaphthylene were a 10 carbon ring-opened product and a dialdehyde, respectively. The major product observed from the API-MS analysis of the O_3 reaction with acenaphthylene was a secondary ozonide, which was not observed by GC-MS.

Introduction

Polycyclic aromatic hydrocarbons (PAHs) are released into the atmosphere during combustion processes. Acenaphthene (I) and acenaphthylene (II) are PAHs emitted into the atmosphere from a variety of sources including diesel exhaust. Under typical ambient temperatures, both compounds exist mainly in the gas phase (*1, 2*) and can thus be removed from the troposphere by gas-phase reaction with hydroxyl (OH) radicals, nitrate (NO_3) radicals, and ozone (O_3) and by photolysis (*3*).

Previous studies have shown that OH radical-initiated reactions with acenaphthene and acenaphthylene are important daylight loss processes in the troposphere (*4*−*7*). Due largely to the presence of the cyclopentafused ring, both compounds also react with NO_3 radicals during nighttime (*4, 8*). Reaction with ozone has also been shown to be an important loss process for acenaphthylene, due to the presence of an unsaturated bond in the cyclopentafused ring (*4*). Although both compounds are expected to have lifetimes in the troposphere of only a few hours, there is some disagreement concerning the rate constants of the gas-phase reactions with the OH radical (*4*−*7*). Therefore, we used relative rate techniques to reexamine those rate constants and that of O_3 with acenaphthylene.

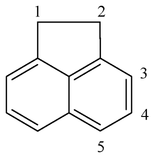

(I)

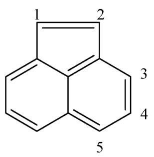

(II)

The mechanisms of the gas-phase reactions of acenaphthene and acenaphthylene with the OH radical and O_3 have not been fully elucidated and only limited product information for these atmospherically important reactions has to date been reported (*5*). In this study, we have used in-situ direct air sampling atmospheric pressure ionization mass spectrometry (API-MS) as well as gas chromatography techniques to investigate the products of the gas-phase reactions of OH radicals with acenaphthene and acenaphthylene and of O_3 with acenaphthylene, including API-MS experiments utilizing acenaphthene-d_{10} and acenaphthylene-d_8.

Experimental Section

Experiments were carried out in ∼6500−7500 L Teflon chambers at 296 ± 2 K and at 740 Torr total pressure of purified air at a relative humidity of ∼5%. The chambers are equipped with a Teflon-coated fan to ensure mixing of the reactants during their introduction into the chamber, two parallel banks of blacklamps for irradiation, and ports for the introduction of reactants and collection of gas samples for analysis. Acenaphthene or acenaphthylene was introduced into the chamber by flowing N_2 gas through a Pyrex tube packed with the solid PAH.

OH radicals were generated by photolysis of methyl nitrite (CH_3ONO) in air at wavelengths >300 nm (*9*). To avoid the formation of O_3, and hence of NO_3 radicals, NO was added to the reactant mixture (*9*). The initial reactant concentrations (in molecule cm^{-3} units) were as follows: CH_3ONO, NO, $\sim 2.7 \times 10^{14}$; *trans*-2-butene, $\sim 2.6 \times 10^{13}$ (in kinetic experiments); and acenaphthene, acenaphthylene, $\sim(1-2) \times 10^{12}$ for reactions with GC analyses; CH_3ONO, NO, $\sim 2.7 \times 10^{13}$; and acenaphthene, acenaphthylene, $\sim(5-10) \times 10^{11}$ for reactions with API-MS analyses.

Ozone was generated using a Welsbach T-408 ozone generator. Each addition of O_3 corresponded to $\sim 6 \times 10^{12}$ molecule cm^{-3} of O_3 in the chamber. The initial reactant concentrations (in molecule cm^{-3} units) were as follows: 2-methyl-2-butene, $\sim 2.6 \times 10^{13}$ (in kinetic experiments); cyclohexane, $\sim 1.3 \times 10^{16}$; and acenaphthylene, $\sim 1 \times 10^{12}$ for reactions with GC analyses; cyclohexane, 8.6×10^{15}; and acenaphthylene, $\sim 5 \times 10^{11}$ for reactions with API-MS analyses.

Kinetic Studies. Rate constants for the reactions of acenaphthene and acenaphthylene with OH radicals and, of acenaphthylene with O_3 were measured using relative rate methods, in which the decay rates of the PAH and a reference

---

* Corresponding author phone: (909)787-3502; fax: (909)787-5004; e-mail: janet.arey@ucr.edu. Corresponding address: Air Pollution Research Center, University of California, Riverside, CA 92521.

† Interdepartmental Program in Environmental Toxicology.

‡ Department of Environmental Sciences.

§ Air Pollution Research Center.

10.1021/es025761b CCC: $22.00

compound, whose rate constant is known, were measured in the presence of OH radicals or O_3 (*4, 10*). Providing that acenaphthene, acenaphthylene, and the reference compound reacted only with OH radicals or O_3, then

$$\ln\left\{\frac{[\mathrm{PAH}]_{t0}}{[\mathrm{PAH}]_{t}}\right\} = \frac{k_1}{k_2}\ln\left\{\frac{[\text{reference organic}]_{t0}}{[\text{reference organic}]_{t}}\right\} \qquad (1)$$

where $[\mathrm{PAH}]_{t0}$ and $[\text{reference organic}]_{t0}$ are the concentrations of the PAH and the reference compound at t_0 and $[\mathrm{PAH}]_t$ and $[\text{reference organic}]_t$ are the concentrations of the PAH and the reference compound at time t; and k_1 and k_2 are the rate constants for reactions 2 and 3, respectively (*4*).

$$\left.\begin{matrix}\mathrm{OH}\\ \mathrm{O_3}\end{matrix}\right\} + \mathrm{PAH} \rightarrow \text{products} \qquad (2)$$

$$\left.\begin{matrix}\mathrm{OH}\\ \mathrm{O_3}\end{matrix}\right\} + \text{reference organic} \rightarrow \text{products} \qquad (3)$$

Plots of $\ln\{[\mathrm{PAH}]_{t0}/[\mathrm{PAH}]_t\}$ versus $\ln\{[\text{reference}]_{t0}/[\text{reference}]_t\}$ should be straight lines with a slope of k_1/k_2 and a zero intercept.

trans-2-Butene was chosen as the reference compound for the OH radical reactions because its rate constant for reaction with OH radicals is similar to those reported for acenaphthene and acenaphthylene (*4*). Three irradiations of 3 min each at 20% of maximum light intensity were carried out, resulting in up to 50% reaction of the initially present acenaphthene and up to 60−65% reaction of the initially present acenaphthylene. Three replicate experiments were done for each PAH.

In the O_3-acenaphthylene reactions, 2-methyl-2-butene was used as the reference compound, and sufficient cyclohexane (1.3×10^{16} molecules cm^{-3}) was added to the chamber to scavenge > 97% of OH radicals formed (*11, 12*). Four additions of 50 cm^3 volume of O_3 in O_2 diluent were made during an experiment. After allowing 8 min for reaction to occur, a sample was collected on a Tenax TA solid adsorbent cartridge for quantitative analysis of acenaphthylene after each addition. Again, three replicate experiments were conducted.

For both the OH radical and O_3 reactions, the reactants were monitored during the experiments by gas chromatography with flame ionization detection (GC-FID). For the analysis of acenaphthene and acenaphthylene, gas samples of 100 cm^3 volume were collected from the chamber onto Tenax TA solid adsorbent cartridges, with subsequent thermal desorption at ~250 °C onto a DB-1701 megabore column. Replicate analyses of acenaphthylene were reproducible, showing no indication of losses to the chamber walls. However, initial experiments with acenaphthene showed a steady drop in concentration over time. Decreasing the initial acenaphthene concentration gave more reproducible results with values typically within 5% (the estimated uncertainty in the GC analyses) over 1.5 h and, therefore, during the less than 2 h required for the acenaphthene kinetic experiments, wall losses were negligible. For the analysis of *trans*-2-butene and 2-methyl-2-butene, gas samples were collected from the chamber in a 100 cm^3 all-glass, gastight syringe and injected via a 1-cm^3 stainless steel loop onto a DB-5 megabore column.

Product Studies. Product analyses were carried out in two series of experiments, with analyses by API-MS in one series and by gas chromatography−mass spectrometry (GC-MS) and GC-FID in another series of experiments.

Reactions with API-MS Analysis. OH radical-initiated reactions of acenaphthene, acenaphthene-d_{10}, acenaphthylene, and acenaphthylene-d_8 and O_3 reactions with acenaphthylene and acenaphthylene-d_8 were carried out in a ~7000 L Teflon chamber directly linked via a Pyrex sampling port to the PE SCIEX API III MS/MS mass spectrometer. The chamber contents were sampled at ~20 L min^{-1} directly into the API-MS source (*13*).

For the OH radical-initiated reactions, the reactants were irradiated at 20% of maximum light intensity for 1 min. For the O_3 reactions, one addition of 50 cm^3 volume of O_3 in O_2 diluent was made to the chamber. The positive ion mode was used in all the API-MS and API-MS/MS analyses, as described in Kwok et al. (*13*).

Reactions with GC Analysis. While sampling on Tenax adsorbent was conducted for analysis of the PAH during the kinetic experiments, sampling both onto Tenax and using solid-phase microextraction (SPME) (*14, 15*) was used for product identification and quantification.

SPME Product Identification and Quantification. Preliminary product analyses were conducted using samples collected during the API-MS experiments for later off-line GC-MS analyses. Conditions for the separate experiments carried out for product identification and quantification were as follows. Irradiations were carried out at 20% of the maximum light intensity for 3 min (1 experiment) and 7 min (2 experiments), resulting in reaction of 52% and 78% of the initially present acenaphthene and for 1.5 min (1 experiment) and 4 min (2 experiments), resulting in 56% and 80% reaction of the initially present acenaphthylene. For the reactions with O_3, two additions of O_3/O_2 mixture were made to the chamber, each addition corresponding to $\sim 6 \times 10^{12}$ molecule cm^{-3} of O_3 in the chamber.

For SPME analysis, a 100 μm poly(dimethylsiloxane) (PDMS) coated fiber was used. The fiber was exposed to the analytes for 30 min, 2 h, and ~16−20 h. Equilibrium of the reactants was reached after 30 min, but longer equilibrium times were required for the products. To have sufficient product signals on the GC-MS and for convenience of sampling, a 16−20 h sampling time was chosen. The sampling process was followed by desorption of the concentrated analytes onto a GC column for analysis. For product identification, a Varian Saturn 2000 GC/MS/MS ion trap was run under chemical ionization (CI) conditions, with isobutane as the reagent gas. Additionally an HP 5971A GC-Mass Selective Detector was run in full scanning mode with electron impact (EI) ionization. The instruments were equipped with a 30 m (Varian Saturn) and a 60 m (HP 5971A) DB-1701 column (0.25 μm phase thickness), and the fiber was thermally desorbed at 250 °C.

For GC-FID quantification with SPME, the fiber was exposed to the chamber contents for 2 and 16 h, subsequently desorbed at 250 °C onto a DB-5 megabore column initially at 40 °C, and then temperature programmed to 280 °C at 8 °C min^{-1}. The amount of analyte that is extracted by the fiber coating when equilibrium has been reached is directly proportional to the analyte concentration in the sample and depends on the volume of the fiber coating and the fiber/sample partition coefficient, as described in ref *16* (refer to Supporting Information for details on product quantification).

Tenax Product Quantification. Product quantification of the OH radical-initiated reaction with acenaphthene was also done using 1 L samples collected on Tenax cartridges and thermally desorbed at 250 °C onto a DB-5 megabore column of a GC-FID. For one experiment with an initial CH_3ONO concentration of 2.7×10^{14} molecule cm^{-3}, three irradiations of 3 min each were carried out at 20% of the maximum light intensity, and for a second experiment with the lower CH_3ONO concentration of 5.5×10^{13} molecule cm^{-3}, three 5 min irradiations were done. The amount of product formed was determined from the analyte peak's area counts based on GC-FID response factors, which were estimated using the calculated ECNs (*17*).

SCHEME 1. OH Radical Addition to a Six-Membered Ring of Acenaphthene[a]

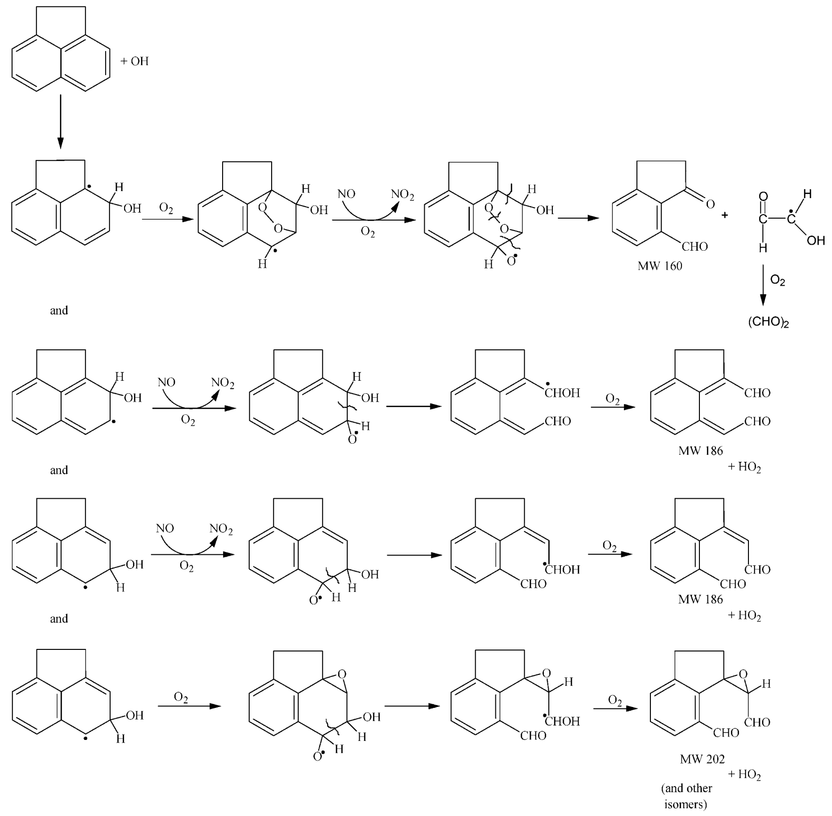

[a] See also Scheme S2, Supporting Information, for formation of additional products by OH radical addition.

TABLE 1. Rate Constant Ratios k_1/k_2 and Rate Constants k_1 for the Gas-Phase Reactions of the OH Radical with Acenaphthene and Acenaphthylene at 296 ± 2 K and Atmospheric Pressure of Air

		$10^{11} \times k$ (cm^3 $molecule^{-1}$ s^{-1})		
PAH	k_1/k_2[a]	this work[a,b]	literature[c]	ref
acenaphthene	1.23 ± 0.06	8.0 ± 0.4	5.8[c]	(*7*)
			10.2 ± 1.2[c]	(*4*)
			6.0 ± 0.8[c,d]	(*6*)
			6.4[e]	(*5*)
acenaphthylene	1.92 ± 0.11	12.4 ± 0.7	10.9 ± 1.1[c]	(*4*)
			12.8[e]	(*5*)

[a] Indicated errors are two least-squares standard deviations. [b] Placed on an absolute basis using a rate constant for the reaction of the OH radical with *trans*-2-butene of $k_2 = 6.48 \times 10^{-11}$ cm^3 $molecule^{-1}$ s^{-1} at 296 K (*12*). Uncertainties in the rate constant k_2 are not taken into account. [c] Updated using the most recent recommendations for the rate constants of the reference compounds (*12*). [d] Rate constant measured over the temperature ranges 325–366 K (*6*). Within the experimental uncertainties, the rate constant is independent of temperature, with the average value cited. [e] Relative to the rate constant for the reaction of the OH radical with naphthalene of 2.2×10^{-11} cm^3 $molecule^{-1}$ s^{-1} at 295 K (*5*).

Particle Formation. Three additional experiments without reference compounds were carried out to investigate the formation of organic aerosols following the oxidation of acenaphthene and acenaphthylene in the presence of OH radicals and the reaction of acenaphthylene with O_3. The particle size distributions were measured using a Scanning Mobility Particle Sizer (SMPS), consisting of a ^{210}Po bipolar charger, a conventional differential mobility analyzer (DMA) (*18, 19*) similar in design to the TSI Model 3934, and a TSI Model 3010 condensation particle counter (CPC). The aerosol flow rate was 1 L min^{-1} and the sheath air flow rate was 3 L min^{-1}. The particle mobility distributions measured with the SMPS were inverted to obtain particle size distributions. The procedure included corrections for particle charging, the DMA function, and the CPC counting efficiency. Details of the general inversion procedure are described in the literature (*20*). The size distributions were used to calculate the total aerosol volume concentration and then multiplied by an assumed particle density of 1 g cm^{-3} to obtain the aerosol mass concentration. The reactant loss was monitored by GC-FID.

SCHEME 2. OH Radical Addition to the Unsaturated Cyclopentafused Ring of Acenaphthylene

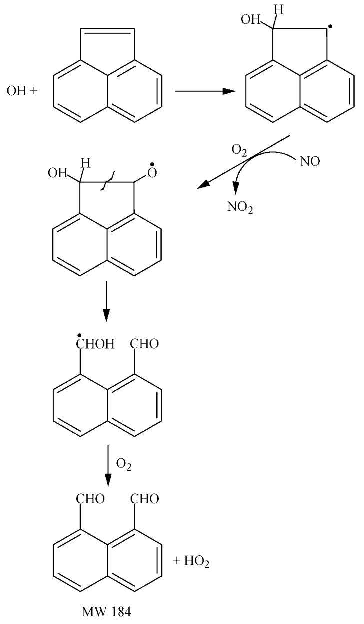

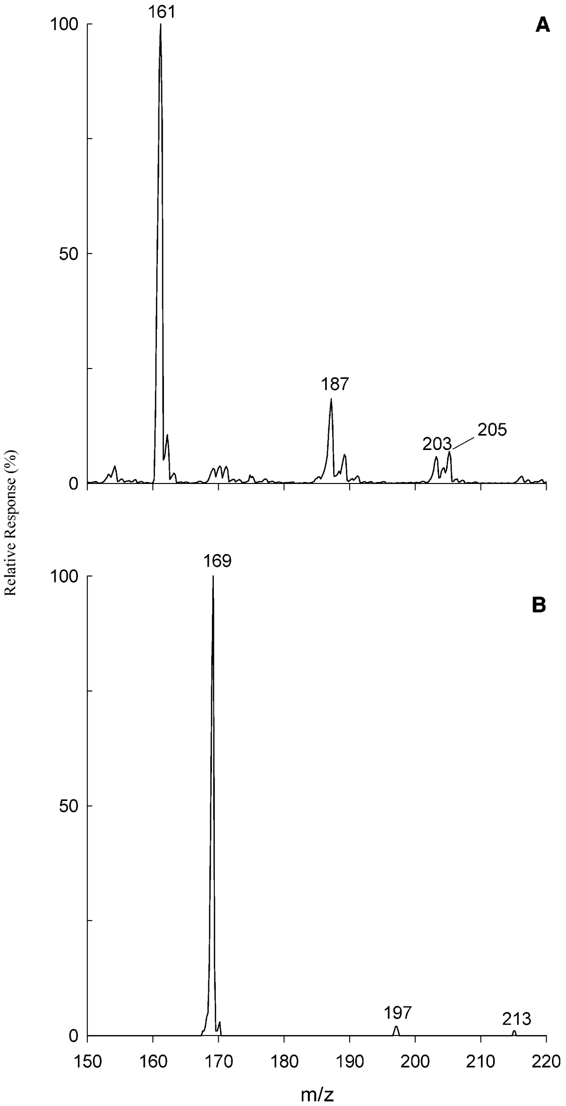

FIGURE 1. API-MS spectra of the gas-phase OH radical-initiated reactions of acenaphthene (A) and acenaphthene-d_{10} (B). See Table 2 for identification of ion peaks.

Chemicals. The chemicals used and their stated purities were as follows: acenaphthene (99%, impurities included acenaphthylene), acenaphthylene (95%, impurities included acenaphthene), 2-methyl-2-butene (99+%) (from Aldrich Chemical Co., St. Louis, MO); acenaphthene-d_{10} (98.7%), acenaphthylene-d_8 (99.7%) (from C/D/N Isotopes Inc.); *trans*-2-butene (95%), NO (>99%), Matheson Gas Products; cyclohexane (HPLC grade) (from Fisher Scientific, Pittsburgh, PA). Methyl nitrite was prepared and stored as described previously (*9*).

Results and Discussion

OH Radical Reaction Rate Constants. The experimental data obtained from irradiated CH_3ONO–NO–PAH-*trans*-2-butene-air mixtures were plotted in accordance with eq 1 (Figure S1, Supporting Information). Reasonable straight-line plots were observed, and the rate constant ratios k_1/k_2 obtained by least-squares analyses of the data are given in Table 1. These ratios are placed on an absolute basis by use of a rate constant k_2 for the OH radical reaction with *trans*-2-butene of $k_2 = 6.48 \times 10^{-11}$ cm^3 molecule^{-1} s^{-1} at 296 K (*12*). The resulting rate constants are also given in Table 1 together with the available literature data.

The rate of the OH radical reaction with acenaphthene has been studied previously (*4*–*7*), but as evident from Table 1, the results of these studies are not in agreement. The reference compound chosen by Klöpffer et al. (*7*) (ethene) was not ideal, as it reacts significantly more slowly than acenaphthene and no uncertainty was cited for their measurement. The Banceu et al. (*5*) study was done relative to naphthalene and used SPME for analysis. Again, no error estimates were reported, and they also reported data for 1,3- and 2,3-dimethylnaphthalenes which are in poor agreement with literature values (*21, 22*), including a recent study of 14 alkylnaphthalenes (*22*). Although outside the stated error limits, the value obtained in this study falls between the rate coefficients determined by Brubaker and Hites (*6*) and by Atkinson and Aschmann (*4*). Brubaker and Hites (*6*) carried out their experiments at elevated temperatures (325–366 K) and extrapolated the data to room temperature. The earlier rate constant measurements from this laboratory (*4*) employed packed column GC techniques, and it is anticipated that our present study using capillary GC columns is more accurate as well as more precise. The rate coefficient obtained in this study is in good agreement with the estimated value of Klamt (*23*) of 8.6×10^{-11} cm^3 molecule^{-1} s^{-1}, which was based on molecular orbital calculations.

The rate coefficient obtained for the OH reaction with acenaphthylene is in agreement with the previous values of Atkinson and Aschmann (*4*) and Banceu et al. (*5*). Acenaphthylene reacts faster with the OH radical than does acenaphthene, presumably due to the higher reactivity of the unsaturated cyclopentafused ring of acenaphthylene.

PAHs react with the OH radical by two reaction pathways: (1) OH radical interaction with the substituent groups, either through H-atom abstraction from a substituent alkyl group, if present, or for those PAHs containing unsaturated cyclopentafused rings, OH radical addition to the $>C{=}C<$ bond; (2) OH-addition to the aromatic ring to form an initially energy-rich hydroxycyclohexadienyl-type radical (*4*).

Acenaphthene and acenaphthylene can each undergo two distinct reaction pathways (see Schemes 1 and 2 and Schemes S1–S3, Supporting Information). As indicated by the products discussed below, addition to the six-membered aromatic rings seems to be the dominant pathway for acenaphthene (Scheme 1), while the faster reaction rate for acenaphthylene suggests that reaction also occurs at the unsaturated bond of the cyclopentafused ring (Scheme 2). Both PAHs react quite rapidly with the OH radical, leading to atmospheric lifetimes with respect to OH radical reactions of 1.8 h for acenaphthene and 1.1 h for acenaphthylene, assuming an average ambient 12-h daytime OH radical concentration of 2×10^6 molecule cm^{-3} (*24, 25*).

O_3 Reaction Rate Constant. The experimental data from a series of O_3-cyclohexane-air-2-methyl-2-butene-acenaphthylene experiments were plotted in accordance with eq 1 (Figure S2, Supporting Information). The rate constant ratio k_1/k_2 obtained by least-squares analyses of the data is 0.395 ± 0.017. This rate constant ratio can be placed on an absolute basis by use of a rate constant k_2 for the reaction of 2-methyl-2-butene with O_3 of $k_2 = 3.96 \times 10^{-16}$ cm^3 molecule^{-1} s^{-1} at 296 K (*12*), and the resulting rate constant for the O_3 reaction with acenaphthylene is $(1.6 \pm 0.1) \times 10^{-16}$ cm^3 molecule^{-1} s^{-1}.

The significant reactivity of acenaphthylene toward O_3 is ascribed to the reaction of O_3 with the unsaturated cyclopentafused ring, since O_3 does not react to any observable extent with aromatic hydrocarbons containing only six-membered rings or with saturated side chains or, as is the case for acenaphthene, saturated cyclopentafused rings (*4*). The rate coefficient determined here is lower than that of Atkinson and Aschmann (*4*), where an approximate rate constant of $k = 5.5 \times 10^{-16}$ cm^3 molecule^{-1} s^{-1} was determined

TABLE 2. Products Observed by API-MS and GC-MS and Their Formation Yields from the Gas-Phase OH Radical-Initiated Reactions of Acenaphthene and Acenaphthene-d_{10}

product		API-MS $[M+H]^+$		GC-MS MW	formation yield [a]
		h_{10}	d_{10}	h_{10}	
$C_{10}H_8O_2$	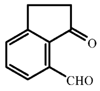	161	169	160	14-37%
$C_{12}H_{10}O_2$ dialdehyde [b]	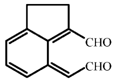	187 [c]	197	186	
$C_{12}H_{10}O_3$	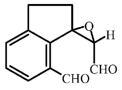	203	213	202	
$C_{12}H_6O_2$ 1,2-acenaphthylenedione [d]	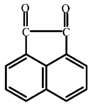			182	
$C_{12}H_6O_3$ 1,8-naphthalic anhydride [d]	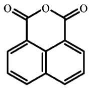			198	
$C_{12}H_9NO_2$ nitroacenaphthene	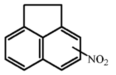			199	

[a] The formation yield has been determined for the MW 160 product, with quantification by Tenax thermal desorption and by SPME (see Supporting Information). [b] GC-MS analysis showed the presence of three isomers of the dialdehyde, which is formed by OH-addition to the aromatic ring. [c] The 205 ion seen in Figure 1A is a water cluster of the 187 ion. [d] Potential artifacts, see text.

under second-order kinetic conditions, with an estimated overall uncertainty of a factor of 2. The present study is the first to use a relative rate method with an OH radical scavenger for the determination of the rate constant of the O_3 reaction with acenaphthylene.

Assuming an ambient O_3 concentration of 7×10^{11} molecules cm^{-3} (30 parts-per-billion, ppbv), which is representative of global lower tropospheric levels (*26*), the rate constant determined in this study results in an atmospheric lifetime of acenaphthylene with respect to O_3 reaction of 2.5 h. This atmospheric lifetime would drop in polluted atmospheres, for example, to 22 min during a California Stage 1 Ozone Episode (O_3 concentration of 200 ppbv).

Products of the Reactions of OH Radicals with Acenaphthene and Acenaphthene-d_{10}. *API-MS Analysis.* Reactions of acenaphthene and acenaphthene-d_{10} with OH radicals in the presence of NO_x were carried out, and the chamber contents were directly sampled and analyzed by API-MS. For acenaphthene, as shown in Figure 1A, three main products were observed by API-MS. The observed products and their suggested structures are listed in Table 2. The major product was tentatively identified as a C_{10} ring-opened product of $[M + H]^+ = 161$. The structure shown in Table 2 is consistent with the $[M + H]^+ = 169$ observed in the acenaphthene-d_{10} reaction (Figure 1B). The second product seen as $[M + H]^+ = 187$ with a water cluster at $[M + H + H_2O]^+ = 205$ is tentatively identified as a dialdehyde, consistent with the presence of 10 nonexchangeable deuteriums in the acenaphthene-d_{10} reaction product. The structure of the third product observed at $[M + H]^+ = 203$, and at $[M + H]^+ = 213$ in the acenaphthene-d_{10} reaction, is suggested to be an epoxide rather than a hydroxy-derivative, since there are 10 nonexchangeable D atoms. Rapid −OD to −OH exchange in the chamber for hydroxy-substituted compounds has been observed (*13*), and, therefore, if the $C_{12}H_{10}O_3$ compound contained an −OH group, only nine nonexchangeable D atoms would be expected, either from −OD/−OH exchange or initial addition of the reactant OH (and not OD) radical. The products seen by API-MS are consistent with those expected from OH radical addition to a six-membered ring of acenaphthene (Scheme 1). The formation of the MW 202 product, shown in the lower pathway in Scheme 1, follows the reaction mechanism proposed by Bartolotti and Edney (*27*). The lack of a significant ion peak at m/z 185, $[M + H]^+$ of naphthalene-1,8-dicarbaldehyde, principal product expected from H-atom abstraction (see Scheme S1, Supporting Information), suggests that H-atom abstraction from the cyclopentafused ring is not important.

GC-MS Analysis. Since the ions that are mass-analyzed are mainly protonated molecular ions, the peaks obtained by API-MS can be matched with the peaks obtained by GC-MS with the CI analyses confirming the molecular ions and EI analyses providing spectra with additional structural information. Figure 2A shows a GC-MS EI total ion chromatogram of an overnight sample collected on a 100 μm PDMS fiber from the gas-phase OH radical-initiated reaction of acenaphthene (78% reaction of the initially present acenaphthene). Single peaks corresponding to the MW 160 and 202 products seen in the API-MS analysis were observed, while three isomers of MW 186 were found (see Scheme 1

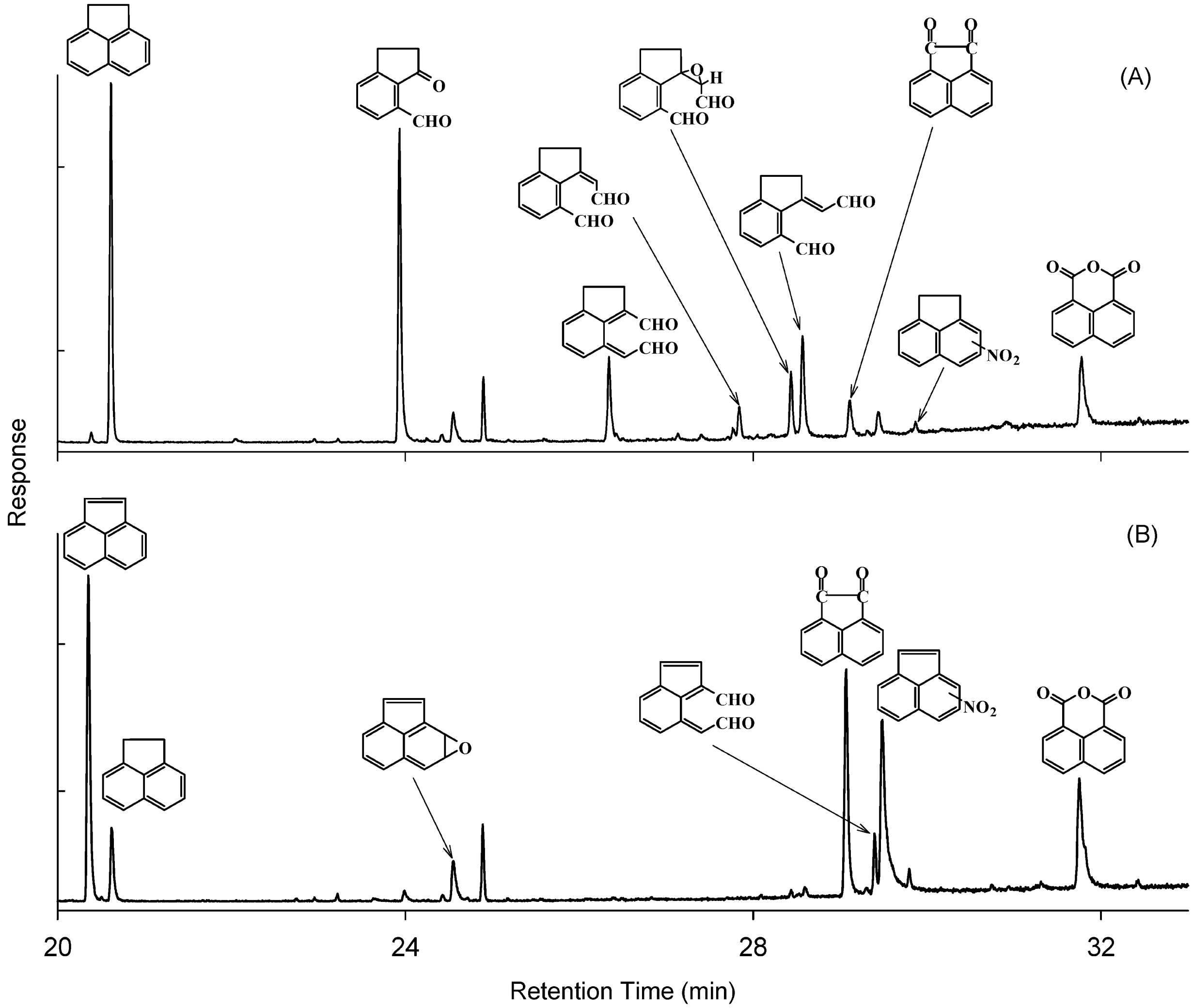

FIGURE 2. GC-MS total ion chromatogram of overnight samples collected on PDMS 100 μm fiber from the gas-phase OH radical-initiated reactions of acenaphthene (A) (7 min irradiation, 78% reaction of initially present acenaphthene) and acenaphthylene (B) (1.5 min irradiation; 56% reaction of initially present acenaphthylene).

for suggested formation pathways). Possible structures of these products are shown in Figure 2A and include cis- and trans-isomers of a ring-opened dialdehyde analogous to *cis*- and *trans*-2-formylcinnamaldehyde, which were identified from the reaction of naphthalene with the OH radical (*28, 29*). The formation of the cis-isomer is shown in Scheme 1, with the trans-isomer potentially formed from photolysis of the cis-isomer (*29*). The EI mass spectra of the suggested dialdehyde products from acenaphthene are consistent with the proposed structures with prominent losses of 29 (CHO) from the molecular ion.

Three additional peaks (see Figure 2A) were observed by GC-MS analysis: a small nitroacenaphthene peak (see Scheme S2, Supporting Information), a peak of MW 182 attributed to 1,2-acenaphthylenedione, and a peak due to 1,8-naphthalic anhydride. From the OH radical-initiated reaction of acenaphthene under similar experimental conditions, low yields (~0.2%) of nitroacenaphthenes have been reported from this laboratory (*8*). Note that hydroxyacenaphthene, a potential product shown in Scheme S2, Supporting Information, was not observed either by GC-MS or API-MS. 1,8-Naphthalic anhydride was found in the GC-MS analyses from reactions of both acenaphthene and acenaphthylene with OH as well as acenaphthylene with O_3 and did not appear in the API-MS analyses of any of these reactions. It is suggested that this stable product forms from more labile products during sampling and analysis. The peak of MW 182 attributed to 1,2-acenaphthylenedione (molecular ion has successive losses of C═O) is believed to be a sampling artifact formed from naphthalene-1,8-dicarbaldehyde during the desorption process (see discussion of acenaphthylene reaction products below). Naphthalene-1,8-dicarbaldehyde could have been present as the reaction product from a small acenaphthylene impurity present in the acenaphthene reactions or, since it would be formed by H-atom abstraction from acenaphthene (see Scheme S1, Supporting Information), it could indicate that this pathway occurred. However, as noted above, naphthalene-1,8-dicarbaldehyde was not observed in the API-MS analyses of the acenaphthene-OH reactions, indicating that H-atom abstraction can be only a very minor pathway.

Product Quantification. Because the MW 160 product was the most prominent in the GC-MS analyses of the SPME samples and of the Tenax samples as well as in the API-MS analyses, an attempt was made to quantify its yield. The amounts of the reactants and products were determined from the peak area counts based on GC-FID response factors. Taking into account secondary reactions, a formation yield of the MW 160 product of ~14% was derived from the experiments where the product was sampled onto Tenax (see Figure S4 and discussion in Supporting Information).

For the quantification with SPME, a maximum yield at 37% was obtained for the 3 min irradiation with a 2 h sampling time after correcting for secondary reactions. The higher yield

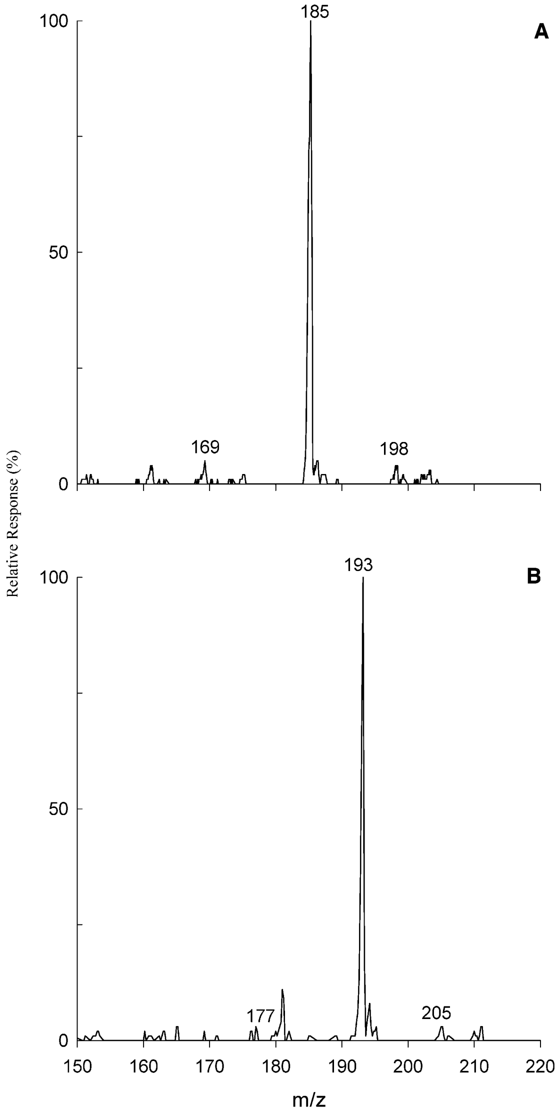

FIGURE 3. API-MS spectra of the gas-phase OH radical-initiated reactions of acenaphthylene (A) and acenaphthylene-d_8 (B). See Table 3 for identification of ion peaks.

determined by SPME suggests the yield measured by Tenax sampling may be an underestimate, but clearly a standard of this product is required to verify quantitative collection and desorption from the Tenax as well as to calibrate the SPME partition coefficient. (Refer to Supporting Information for details on quantification and estimation of the product partition coefficient).

Products of the Reactions of OH Radicals with Acenaphthylene and Acenaphthylene-d_8. *API-MS Analysis.* Reactions of acenaphthylene and acenaphthylene-d_8 with OH radicals in the presence of NO_x were carried out, and the chamber contents were directly sampled and analyzed by API-MS. For acenaphthylene, as shown in Figure 3A, one product dominated. The products observed by API-MS and their suggested structures are shown in Table 3. Unlike acenaphthene, where addition to the ring and H-atom abstraction are predicted to give different molecular weight dialdehyde products, both OH addition to the cyclopentafused ring and to the aromatic rings of acenaphthylene are predicted to give dialdehydes of MW 184 (see Scheme 2 and Scheme S3, Supporting Information). As shown in Figure 3A, the API-MS analysis is indeed dominated by a product peak at $[M + H]^+ = 185$ suggested to be a dialdehyde and consistent with the $[M + H]^+ = 193$ in the acenaphthylene-d_8 reaction (Figure 3B).

Other product ion peaks were observed at 169 and 198 (acenaphthylene) and 177 and 205 (acenaphthylene-d_8). The ion peaks at 169 and 177 u, respectively, indicate the presence of eight nonexchangeable H atoms, and, therefore this compound is attributed to an epoxide rather than a hydroxy-derivative. The third product at $[M + H]^+ = 198$ was identified as a nitro-derivative, consistent with the seven deuteriums in the acenaphthylene-d_8 reaction (Figure 3B). A 2% yield of 4-nitroacenaphthylene from the reaction of OH with acenaphthylene has previously been reported from this laboratory (*8*).

GC-MS Analysis. Figure 2B shows a GC-MS total ion chromatogram of an overnight sample collected on a 100 μm PDMS fiber from the gas-phase OH radical-initiated reaction of acenaphthylene (56% reaction of the initially present acenaphthylene). Possible structures for five products suggested by their MS EI spectra are shown next to the GC peaks. Consistent GC-MS analysis results for the acenaphthylene products were not obtained. The 1,2-acenaphthylenedione peak (with distinctive successive losses of 28 and 28 from the molecular ion) was the largest peak observed in the analysis shown in Figure 2B. At other times, the 1,2-acenaphthylenedione peak was small, and two molecular weight 184 dialdehydes were observed. The relative proportions of the peaks found for the two MW 184 products and the MW 182 peak suggest that one of the MW 184 products decomposed to the dione. OH radical addition to the unsaturated cyclopentafused ring is expected to yield naphthalene-1,8-dicarbaldehyde (see Scheme 2), consistent with the API-MS analyses. It is proposed, therefore, that naphthalene-1,8-dicarbaldehyde is susceptible to degradation to 1,2-acenaphthylenedione during GC analysis, perhaps during the analyte desorption in the heated inlet. Consistent with the API-MS analyses, an epoxide of MW 168 and nitroacenaphthylene were observed. As noted previously, 1,8-naphthalic anhydride was again observed, while no corresponding molecular ion peak was seen in the API-MS analyses.

The reactivity, and double-bond character, of the unsaturated cyclopentafused ring of acenaphthylene is demonstrated by its reaction with O_3. Therefore the presence of two different MW 184 products suggests that both OH addition to the cyclopentafused ring (Scheme 2) and to the aromatic rings of acenaphthylene (see Scheme S3, Supporting Information) must occur.

Products of the Reactions of O_3 with Acenaphthylene and Acenaphthylene-d_8. *API-MS Analysis.* API-MS positive ion analyses of O_3 with acenaphthylene and acenaphthylene-d_8 were carried out, and the spectra of these reactions showed the presence of a single dominant product ion peak $[M + H]^+$ at 201 and 209 u, respectively (see Figure S3, Supporting Information for the API-MS/MS CAD spectra of these ion peaks). The CAD spectra of both compounds show losses of OH, CO, and 2CO. Additionally, the acenaphthylene reaction product peak shows losses of $CO + H_2O$, while the acenaphthylene-d_8 product peak shows corresponding losses of $CO + HDO$. Thus, as evidenced by eight nonexchangeable hydrogens and the addition of 48 mass units in the product peak, in-situ API-MS analysis allowed identification of the secondary ozonide (see Table 4 for structure).

GC-MS Analysis. As shown in Table 4, the GC-MS analysis of the acenaphthylene reaction with O_3 showed six apparent products: 1-naphthaldehyde, oxaacenaphthylen-2-one, 2-hydroxy-1-naphthaldehyde, two dialdehydes of MW 184, and 1,8-naphthalic anhydride. The secondary ozonide was not observed by GC-MS, and the products observed are, therefore, attributed to breakdown products of the secondary ozonide.

TABLE 3. Products Observed by API-MS and GC-MS from the Gas-Phase OH Radical-Initiated Reactions of Acenaphthylene and Acenaphthylene-d_8

product		API-MS $[M+H]^+$ h_8	API-MS $[M+H]^+$ d_8	GC-MS MW h_8
$C_{12}H_8O$ epoxide	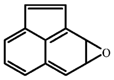	169	177	168
$C_{12}H_8O_2$ naphthalene-1,8-dicarbaldehyde [a]	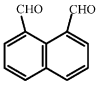 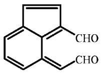	185	193	184
$C_{12}H_7NO_2$ nitroacenaphthylene	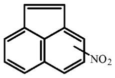	198	205	197
$C_{12}H_6O_2$ 1,2-acenaphthylenedione [b]	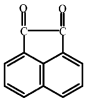			182
$C_{12}H_6O_3$ 1,8-naphthalic anhydride [b]	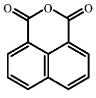			198

[a] Naphthalene-1,8-dicarbaldehyde is formed by OH addition to the unsaturated bond at the cyclopentafused ring. Dialdehydes of MW 184 can also be formed by OH addition to the aromatic ring. [b] Potential artifacts, see text.

Overall Reactions, Product Mass Balances, and Particle Formation. As a result of the short atmospheric lifetimes for both acenaphthene and acenaphthylene, their products are likely to be present in ambient air and therefore the toxicity of these products is of concern. Carbonyl compounds were the major products observed here, and unsaturated aldehydes and dicarbonyl compounds have been shown to react with DNA (*30, 31*). Muconaldehyde, a six-carbon diene dialdehyde, has been shown to be genotoxic (*32*). Additionally, epoxides have been identified from the OH radical reactions of both acenaphthene and acenaphthylene, and epoxy functional groups have been shown to act as electrophiles and react with DNA (*33*−*35*).

For the OH radical-initiated reactions of acenaphthene and acenaphthylene, product mass balances were not obtained. Quantification by API-MS was not possible due to the lack of standards for the products and this lack necessitated using GC-FID, where the detector response can be predicted (*17*), for quantification. However, no assessment of quantitative recovery during sampling and GC analysis could be made. The major product from acenaphthene (MW 160) accounted for ∼14−37% of the OH radical reaction products, whereas the dialdehyde product of the OH reaction with acenaphthylene accounted for even less. The experiments that were carried out indicate that organic aerosol formation following the OH radical-initiated reaction of acenaphthene and acenaphthylene was not significant, being <1%. Since aerosol formation has proven to be insignificant and it is believed that the API-MS will respond to all reaction products (though with varying sensitivities), wall losses and/or difficulties in quantitative sampling and analysis must explain the low mass balances obtained.

The products observed from the OH reaction of acenaphthene suggest that addition to the aromatic ring dominates over H-atom abstraction from the cyclopentafused ring. This is consistent with expectations that ∼60% of reactivity for acenaphthene arises from the 4 and 5 positions (*23*) but inconsistent with the study of Banceu et al. (*5*), in which a high proportion of the proposed products are formed by reaction at the saturated cyclopentafused ring. For acenaphthylene, Klamt (*23*) estimated that reaction at the unsaturated bond of the cyclopentafused ring accounts for the majority of reactivity. Again this is consistent with the products observed here from the OH reaction with acenaphthylene. Although API-MS analysis cannot distinguish isomers, a dialdehyde peak totally dominated the spectrum, and GC analyses suggested that mainly naphthalene-1,8-dicarbaldehye was formed (observed as the dialdehyde or as 1,2-acenaphthylenedione). The formation of naphthalene-1,8-dicarbaldehyde would result from addition to the cyclopentafused ring (Scheme 2), while the presence of a second less abundant dialdehyde suggests some reaction with the aromatic ring also occurred (see Scheme S3, Supporting Information).

The formation of organic aerosol following the reaction of O_3 with acenaphthylene accounted for ∼13% of the product mass balance. The secondary ozonide, the only product observed in the API-MS analyses, presumably accounts for a large fraction of the overall reaction products. The secondary ozonide was clearly unstable in our off-line GC analyses, and it is not known what the fate of the secondary ozonide would be under ambient conditions.

TABLE 4. Products Observed by API-MS and GC-MS from the Gas-Phase O_3 Reactions of Acenaphthylene and Acenaphthylene-d_8

product		API-MS $[M+H]^+$ h_8	d_8	GC-MS MW h_8
$C_{12}H_8O_3$ secondary ozonide	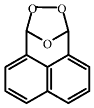	201	209	Not observed
$C_{11}H_8O$ 1-naphthaldehyde	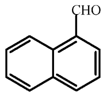			156
$C_{11}H_6O_2$ oxaacenaphthylen-2-one	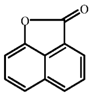			170
$C_{11}H_8O_2$ 1-naphthaldehyde, 2-hydroxy	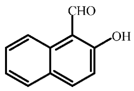			172
$C_{12}H_8O_2$ naphthalene-1,8-dicarbaldehyde	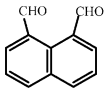			184
$C_{12}H_8O_2$ dialdehyde	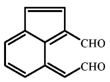			184
$C_{12}H_6O_3$ 1,8-naphthalic anhydride	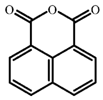			198

Acknowledgments

The authors thank Dr. Roger Atkinson for many helpful discussions and Dr. Paul Ziemann for loaning us the equipment and providing us with the expertise required to measure particle formation. The authors gratefully thank the U.S. Environmental Protection Agency through Grant No. R826371-01-0 “Ozone and Fine Particle Formation in California and in the Northeastern United States” to the California Institute of Technology for support of this research. One of the authors (F.R.) has been partially supported by a grant from the University of California Toxic Substances Research & Teaching Program. While this research has been supported by the U.S. EPA, it has not been subjected to Agency review and, therefore, does not necessarily reflect the views of the Agency.

Supporting Information Available

Figures S1−S4 and reaction Schemes S1−S3 and information on product quantification with SPME and Tenax TA solid adsorbent and the yield determination for the MW 160 product. The materials are available free of charge via the Internet at http://pubs.acs.org.

Literature Cited

(1) Bidleman, T. F.; Billings, W. N.; Foreman, W. T. *Environ. Sci. Technol.* **1986**, *20*, 1038−1043.
(2) Cousins, I. T.; Mackay, D. *Environ. Sci. Technol.* **2001**, *35*, 643−647.
(3) Atkinson, R. *Atmos. Environ.* **2000**, *34*, 2063-2101.
(4) Atkinson, R.; Aschmann, S. M. *Int. J. Chem. Kinet.* **1988**, *20*, 513−539.
(5) Banceu, C. E.; Mihele, C.; Lane, D. A.; Bunce, N. J. *Polycyclic Aromat. Compd.* **2001**, *18*, 415−425.
(6) Brubaker, W. W., Jr.; Hites, R. A. *J. Phys. Chem. A* **1998**, *102*, 915−921.
(7) Klöpffer, V. W.; Frank, R.; Kohl, E.-G.; Haag, F. *Chemiker-Zeitung* **1986**, *110*, 57−61.
(8) Arey, J.; Zielinska, B.; Atkinson, R.; Aschmann, S. M. *Int. J. Chem. Kinet.* **1989**, *21*, 775−799.
(9) Atkinson, R.; Carter, W. P. L.; Winer, A. M.; Pitts, J. N., Jr. *J. Air Pollut. Control Assoc.* **1981**, *31*, 1090−1092.
(10) Greene, C. R.; Atkinson, R. *Int. J. Chem. Kinet.* **1992**, *24*, 803−811.
(11) Alvarado, A.; Atkinson, R.; Arey, J. *Int. J. Chem. Kinet.* **1996**, *28*, 905−909.
(12) Atkinson, R. *J. Phys. Chem. Ref. Data* **1997**, *26*, 215−290.
(13) Kwok, E. S. C.; Arey, J.; Atkinson, R. *J. Phys. Chem.* **1996**, *100*, 214−219.

(14) Pawliszyn, J. *Solid-Phase Microextraction: Theory and Practice*; Wiley-VCH: New York, 1997.
(15) Pawliszyn, J. *Applications of Solid-Phase Microextraction*; Royal Society of Chemistry: Cambridge, 1999.
(16) Martos, P. A.; Saraullo, A.; Pawliszyn, J. *Anal. Chem.* **1997**, *69*, 402−408.
(17) Scanlon, J. T.; Willis, D. E. *J. Chromatogr. Sci.* **1985,** *23*, 333−340.
(18) Knutson, E. O. *J. Aerosol Sci.* **1975**, *6*, 443−451.
(19) Liu, B. Y. H.; Pui, D. Y. H. *J. Colloid Interface Sci.* **1974,** *47*, 155−171.
(20) Wang, S. C.; Flagan, R. C. *Aerosol Sci. Technol.* **1990**, *13*, 230−240.
(21) Atkinson, R.; Aschmann, S. M. *Atmos. Environ.* **1987**, *21*, 2323−2326.
(22) Phousongphouang, P. T.; Arey, J. *Environ. Sci. Technol.* **2002**, *36*, 1947−1952.
(23) Klamt, A. *Chemosphere* **1993**, *26*, 1273−1289.
(24) Hein, R. Crutzen, P. J.; Heimann, M. *Global Biogeochem. Cycle* **1997**, *11*, 43−76.
(25) Prinn, R. G.; Weiss, R. F.; Miller, B. R.; Huang, J.; Alyea, F. N.; Cunnold, D. M.; Fraser, P. J.; Hartley, D. E.; Simmonds, P. G. *Science* **1995**, *269*, 187−192.
(26) Logan, J. A. *J. Geophys. Res.* **1985**, *90*, 10463−10482.
(27) Bartolotti, L. J.; Edney, E. O. *Chem. Phys. Lett.* **1995**, *245*, 119−122.
(28) Bunce, N. J.; Liu, L.; Zhu, J.; Lane, D. A. *Environ. Sci. Technol.* **1997**, *31*, 2252−2259.
(29) Sasaki, J.; Aschmann, S. M.; Kwok, E. S. C.; Atkinson, R.; Arey, J. *Environ. Sci. Technol.* **1997**, *31*, 3173−3179.
(30) Marnett, L. J.; Hurd, H. K.; Hollstein, M. C.; Levin, D. E.; Esterbauer, H.; Ames, B. N. *Mutat. Res.* **1985**, *148*, 25−34.
(31) Marnett, L. J. In *DNA Adducts: Identification and Biological Significance*; Hemminki, K., Dipple, A., Shuker, D. E. G., Kadlubar, F. F., Segerbäck, D., Bartsch, H., Eds.; International Agency for Research on Cancer: Lyon, 1994; Vol. 125, pp 151−163.
(32) Witz, G.; Gad, S. C.; Tice, R. R.; Oshiro, Y.; Piper, C. E.; Goldstein, B. D. *Mutat. Res.* **1990**, *240*, 295−306.
(33) Ehrenberg, L.; Hussain, S. *Mutat. Res.* **1981**, *86*, 1−113.
(34) Hemminki, K. *Arch. Toxicol.* **1983**, *52*, 249−285.
(35) Segerbäck, D. In *DNA Adducts: Identification and Biological Significance*; Hemminki, K., Dipple, A., Shuker, D. E. G., Kadlubar, F. F., Segerbäck, D., Bartsch, H., Eds.; International Agency for Research on Cancer: Lyon, 1994; Vol. 125, pp 37−47.

Received for review May 1, 2002. Revised manuscript received July 23, 2002. Accepted July 25, 2002.

ES025761B